Develop, Test and Model a Space Suit Simulator

Ivo Ferreira

Instituto Superior Técnico, Av. Rovisco Pais, 1049-001 Lisboa, Portugal

15th October 2007

Abstract

The torques required to move the joints of a spacesuit are complicated nonlinear functions changing depending on the position and the displacement speed of the joint. Uncertainty in the knowledge of these torques leads to great variations of the metabolic costs of the astronaut and thus, reduces the performance of the EVA.
This is the reason why currently the real spacesuits are used for planning this type of activities.
The use of a simulator to plan EVAs will allow a reduction of the planning procedures costs, a simplification of the training procedure of the astronauts and a better study of the influence of the various parameters of a spacesuit on the behavior of the astronaut.
This thesis describes the procedure that allowed the characterization of the knee joint of this simulator in terms of the sensitivity to the displacement speed, angle range, friction and stiffness.
To better understand the effect of a change on the joint stiffness, a physical model of the joint was built. Also, to predict the hysteretic behavior of the joint, a new model, based on the Bouc-Wen model was built.

1. Introduction

1.1. Context and Motivation

Astronauts and cosmonauts have made great accomplishments while working outside of their spacecraft, assembling and maintaining space stations, capturing and repairing satellites and even exploring the Moon. When astronauts exit their spacecraft to perform Extravehicular Activities, or EVA's, these operations carry extremely high costs in time, money, risks to personnel, and limited opportunities. Because of the high costs of EVA and the importance of accomplishing planned objectives, months of prior planning and hundreds of hours of rehearsal are required to prepare for each EVA. Planning for EVAs is complicated by the fact that it is not possible to exactly replicate the microgravity, vacuum environment in a single simulation environment on the ground. Thus, successful planning for EVA's requires accurate knowledge of the EVA environment and the capabilities of an astronaut wearing a spacesuit.

The number of EVAs increases since the beginning of the space race, and the tendency is to continue increasing.

1.2. Scope of the project

The NASA Johnson Space Center Exercise Countermeasure Project and EVA Physiology Systems and Performance Project are developing a Space Suit Simulator (S3) to substitute for an actual spacesuit during certain types of tests and experiments. The space suit simulator is intended to replicate the mechanical properties of a spacesuit, in terms of resistance to motion and mass and inertia, but without the requirements for pressurization or thermal regulation. This capability will provide several advantages over testing with an actual spacesuit:

1. Reduces cost by eliminating the need for support personnel and consumables associated with actual spacesuits.
2. Eliminates the cost and programmatic impact associated with consumption of suit life due to high cycle testing.
3. Simplifies scheduling since suit simulators will be more readily available than actual spacesuits.
4. Facilitates the use of instrumentation (e.g., metabolic gas analysis, electromyography) that is otherwise difficult or infeasible to implement when using an actual spacesuit.
5. Allows for variation of suit properties to assess the impacts of specific suit parameters (e.g., suit mass, joint resistance, etc.)

The concept that is proposed for the space suit simulator is an exoskeleton-type suit that utilizes commercial-off-the-shelf joint braces, to which are added passive resistance elements, such as bungees and springs, and mass elements that provide the required resistance to motion. The suit joints will be linked-together in a kinematic chain that matches that of the human body using adjustable frame elements. The complete suit will include the following 10 joints with associated degrees of freedom:

- 2 ankle joints, allowing 3 degrees of freedom (rotation, inversion and flexion)
- 1 knee joint, allowing 1 degree of freedom (flexion)
- 2 hip joints, allowing 3 degrees of freedom (flexion, abduction and rotation)
- 1 torso joint, allowing 1 degree of freedom (rotation)
- 2 shoulder joints, allowing 3 degrees of freedom (rotation, flexion and abduction)
- 1 elbow joint, allowing 1 degree de freedom (flexion).

This project is divided in four phases related to the development and test of the space suit simulator:

- Phase I - Knee Joint
- Phase II - Add ankle and hip to complete right leg, plus lower torso
- Phase III - Shoulder and elbow for right arm, plus upper torso
- Phase IV - Complete opposite side arm and leg and integrate complete suit

This thesis describes the procedure developed to test, model and validate the design of the simulator and reveals the first results for the Phase I of the project (knee joint).

Figure 1 - Artist View of the Space Suit Simulator (S3)

2. Testing Tools

One important shortcoming of current EVA models is that they lack an accurate representation of the torques that are required to bend the joints of the spacesuit. Modern spacesuits are designed to move with astronauts, using bearings and constant-volume joints to minimize resistance to motion. However, the torques required to perform EVA tasks still have a significant impact on task performance. The torques required to move spacesuit joints are complicated nonlinear functions of joint position and rate. Uncertainty in the knowledge of these torques leads to large variations in predicted task performance and metabolic costs.

This problem forced NASA to launch, in the 90's, a project for the development of a robot with the same essential degrees of freedom of a human person to be able to measure in an exact way the torques required for various configurations of positioning and rate of travel of the articulations.

2.1. The Robotic Space Suit Tester (RSST)

The RSST is an anthropomorphic robot whose primary purpose is to measure the joint torques exerted by a spacesuit on a human wearer.

The RSST has 12 hydraulically actuated joints on the right arm and leg and 12 poseable joints on the left arm and leg. At each actuated joint, potentiometers measure joint deflection and strain gauge load cells measure torque.

The next picture shows the different joints of the robot:

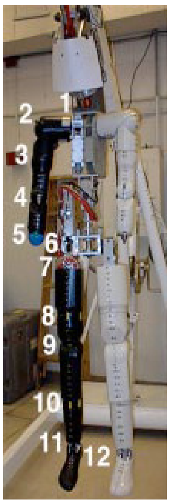

Figure 2 - Joints of the RSST

Number	Description
1	Shoulder Flexion
2	Shoulder Abduction
3	Humerus Rotation
4	Elbow Flexion
5	Wrist Rotation
6	Hip Flexion
7	Hip Abduction
8	Thigh rotation
9	Knee Flexion
10	Ankle Rotation
11	Ankle Flexion
12	Ankle Inversion

Table 1 - Description of the different joints of the RSST

2.2. Choice of the Data Acquisition Boards (DAQ)

The selected connection to input trajectories into the robot and to receive telemetry from the robot was USB and the acquired boards were of two distinct companies:
- Data Translation DT9814-10V, having 24 analogical inputs with a resolution of 12 bits with a frequency of 50 KHz; and,
- Measurement Computing USB-3105, having 16 analogical outputs with a resolution of 16 bits with a frequency of 100 Hz.

2.3. Software to interface with the robot

The choice of the use of Matlab, in particular Simulink, allowed the use of the DAQ Toolbox. This tool transformed the integration of the boards in an easy task because there were already "blocks" to represent the various inputs and outputs of the boards in a model of Simulink.
The only thing missing was a control system and an interface between the user-defined trajectories and the analog outputs.
To address this matter a Simulink model was developed to linearly transform a position in a voltage (according to the maximum/minimal range of the joint and maximum/minimal voltage of the outputs) in the following way:

$$Voltage\_ouput\ (Position) = Minimum\_Voltage + \frac{Position - Minimum\_Position}{Maximum\_Position - Minimum\_Position} \times (Maximum\_Voltage - Minimum\_Voltage)$$

Equation 2

The same type of conversion was used to analyze the telemetry coming from the robot.

3. Data analysis and treatment

3.1. Load Trajectories

The user can either create a **user-defined trajectory** for each joint, **load a human trajectory**, or input parameters that will **generate trajectories for hysteresis graphs with different ranges of motion**, like those shown in the next figure:

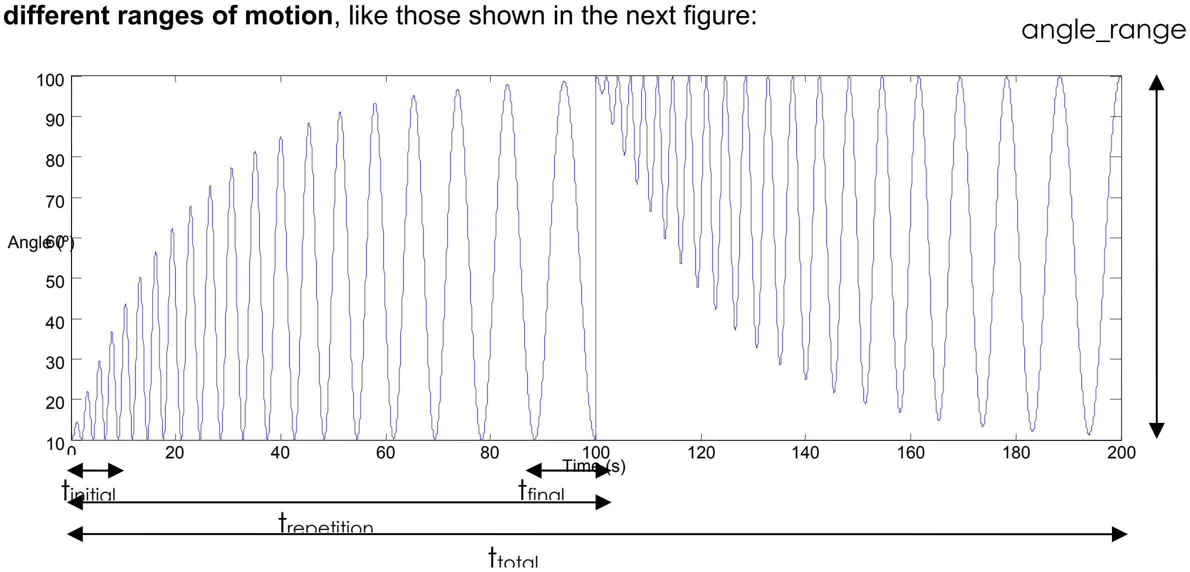

Figure 3 - Example of trajectory to generate hysteresis graphs with different ranges of motion

3.2. Data filtering

The data output from the robot is very noisy, so there was a need to apply a filter before plotting each result.

Collected angle and torque data were Butterworth filtered (10^{th} order filter with a cut-off frequency of 10% of the padding frequency) to remove noise and processed to remove the transition region (the part of the data that corresponded to the robot leg moving into its initialization position).

3.3. Remove torque generated by the robot

In order to measure the effect the spacesuit simulator has on the joints, the torque generated by the robot's weight needs to be subtracted from the raw robot output data. This was not a straight-forward task.

3.3.1. Detection of transition phase

The sensors have a transitory phase that has to be identified and eliminated. This was accomplished by comparing the input trajectory with the output position and searching the point where the difference between these two functions was within five degrees. This was done by comparing three different points after the possible point of transition: when all these points where within that margin, then the transition point had been reached.

3.3.2. Scaling procedure

The trajectory used to test the robot and the spacesuit simulator joint cannot be used directly to measure the torque due to the robot's weight (because the output angles are considerably different between trials with and without the physical joint brace). The only reliable method to remove the robot's torque from the collected data is to use the output trajectory (in angles) and feed it as an input trajectory to the robot. Through this method, torques are compared at the same angles. However, there is a difference between the input and the output angles in general. Thus, the input angles in the trial without the spacesuit simulator joint had to be scaled appropriately so that the output angles are the same as the trial with the spacesuit simulator joint. This scale was simply:

$$Scale = \frac{Max\_angle\_with\_joint - Min\_angle\_with\_joint}{Max\_angle\_without\_joint - Min\_angle\_without\_joint}$$

Equation 2

The new input angles for the trial without the brace were found by the following iterative procedure:

$$\begin{cases} \alpha_{input\_without\_brace\_scaled}{}^{0} = \alpha_{input\_without\_brace\_not\_scaled}{}^{0} \\ \alpha_{input\_without\_brace\_scaled}{}^{i} = \alpha_{input\_without\_brace\_scaled}{}^{i-1} + \\ scale \times (\alpha_{input\_without\_brace\_not\_scaled}{}^{i} - \alpha_{input\_without\_brace\_not\_scaled}{}^{i-1}) \end{cases}$$

Equation 3

4. The Knee joint

The knee joint of the space suit simulator would need to be, according to NASA's statement of work, adjustable in terms of:
- Range of maximum angles,
- Friction,
- Stiffness.

Here is the design that implemented the necessary adaptability:

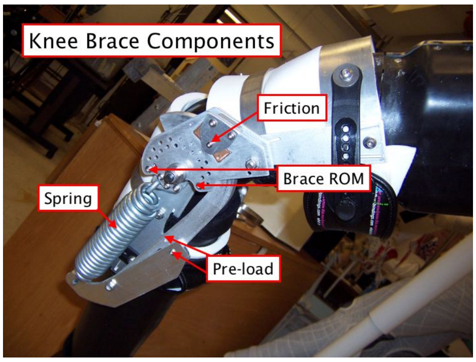

Figure 4 - Knee flexion joint of the space suit simulator

Note: The change of the stiffness of the joint was accomplished by changing the spring at its pre-load.

5. Results

As stated in the Introduction, the scope the testing procedure specified in the work plan was as follows:

- Characterize the sensitivity of the joint torque versus angle relationship on joint displacement speed.
- Characterize the hysteresis behavior of the joint.
- Quantify the adjustability of joint range of motion.
- Quantify the adjustability of joint friction.
- Quantify the adjustability of joint stiffness.

The knee joint was attached in a way that prevented relative motion of the brace on the upper attachment. Since the axis of rotation of the joint was not aligned with the axis of rotation of the robot knee, the joint slid up and down on the lower attachment (back of the calf). The joint was adjusted to cross the zero torque value at an angle of 20°.

Testing results for these five parameters are presented in this section.

5.1. Sensitivity of the joint torque versus angle relationship to joint displacement speed

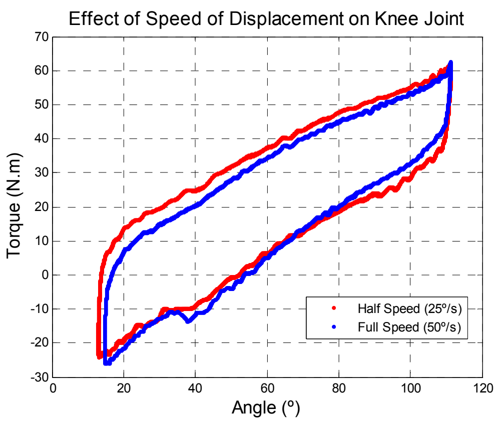

Figure 5 - Difference in the same trajectory run at 25°/s (half) speed and 50°/s (full) speed.

Adjusting trajectory speed has little effect on maximum joint torques.

5.2. Sensitivity of the joint torque versus angle relationship to the limitation of the joint range of motion

Three configurations of the knee joint were tested, one without any limitation of the range of motion [0º,130º], and two smaller ranges ([20º,110º] and [40º,90º]).

Figure 6 - Effect of the limitation of the range on the hysteresis graph of the knee joint

Joint range of motion limits were set by manually setting the position of four screws (**Erro! A origem da referência não foi encontrada.**4). Despite the well-calibrated position of these screws in the knee joint, the robot was still able to move beyond these limits because the knee brace axis of rotation does not align with the robot knee axis of rotation, but in these ranges the robot must "fight" the extra resistance force from the joint.

5.3. Sensitivity of the joint torque versus angle relationship to the friction

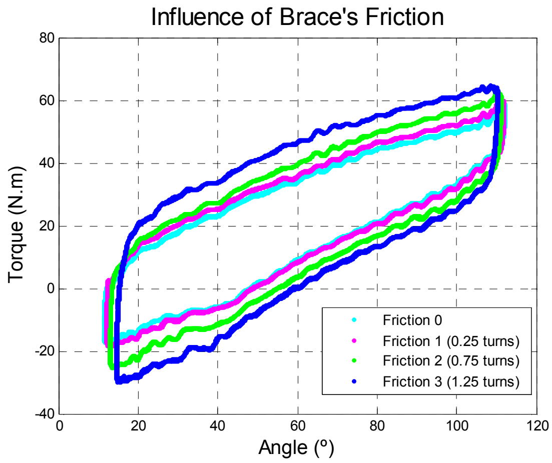

Figure 7 - Effect of friction on the torque vs. angle graph of the knee joint

As expected, the area of the graph visibly increases with the friction, suggesting that the energy loss increases with increasing friction.

5.4. Sensitivity of the joint torque versus angle relationship to the stiffness

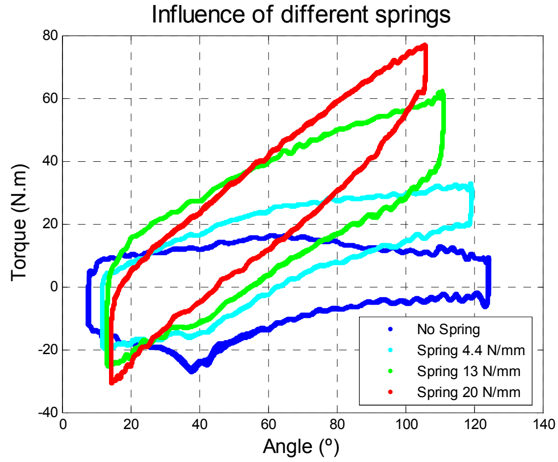

Figure 8 - Effect of stiffness on the hysteresis graph of the knee joint

As expected, increasing the spring stiffness of the knee joint resulted in a change of the slope of the torque vs. angle graph.

5.5. Sensitivity of the joint torque versus angle relationship to the preload

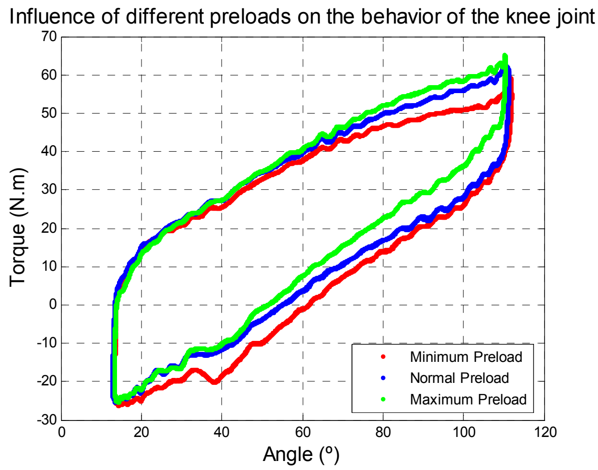

Figure 9 - Effect of preload on the hysteresis graph of the knee joint

Although the effect of a change on the preload of the knee joint is not linear, as is detailed in the Model section of this article, it can be seen that by increasing the preload, the slope of the torque vs. angle graph also increases.

6. Models

6.1. Physical Model

A physical model was built to understand the effects of using different springs and preloads, using an angle parameterization of the knee joint.

Here is the result of the comparison between the real data and the physical model:

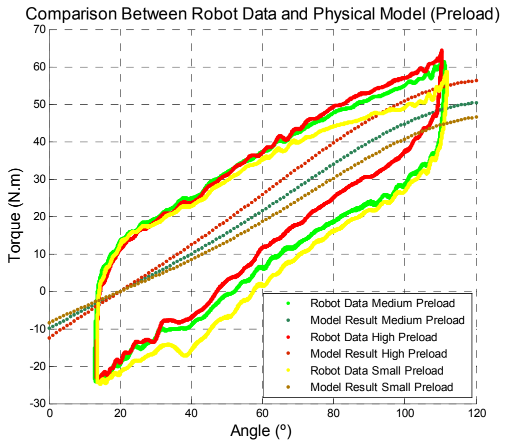

Figure 10 - Effect of a preload change (comparison with real data)

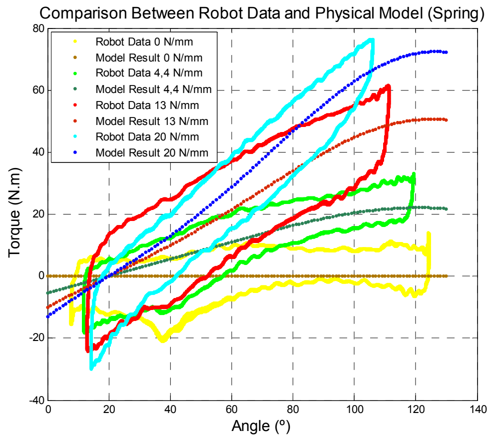

Figure 11 - Effect of a spring change (comparison with real data)

6.2. Mathematical Model

Since the physical model could not explain the hysteretic effect of the joint, a new model, this time a mathematical one, was developed.

6.2.1. The Bouc-Wen model

This model has the advantage of being easy to implement by means of computer, because only one auxiliary nonlinear equation is necessary to describe the hysteresis.

For a structural element ruled by a Bouc-Wen hysteretic model, the resisting force can be defined in the following way:

$$f_s(x,\dot{x},z) = \alpha K_0 x + (1-\alpha) K_o z$$

Equation 4

Where *x* represents position, $\dot{x}$ =*dx*/*dt* is the speed of displacement, α is the coefficient that represents the elastic behavior proportion (if α = 1, the resisting force is fully elastic), K_0 is the initial stiffness and *z* is an auxiliary variable that represents the inelastic behavior.
The evolution on z follows the following ordinary differential equation:

$$\dot{z} = \dot{x}\left[A - |z|^n \Psi(x,\dot{x},z) \right]$$

Equation 5

Where $\dot{z}$ =*dz*/*dt* is the virtual speed of displacement of *z*; *A* and *n* are parameters that control the scale and stiffness of the different hysteresis loops; $\Psi(x,\dot{x},z)$ is a non linear function of *x*, $\dot{x}$ and *z* that the controls the shape of the hysteresis loops.

The following $\Psi(x,\dot{x},z)$ function was created to allow an asymmetric hysteretic behavior:

$$\Psi(x,\dot{x},z) = \beta_1 \operatorname{sgn}(\dot{x} z) + \beta_2 \operatorname{sgn}(\dot{x} x) + \beta_3 \operatorname{sgn}(xz) + \beta_4 \operatorname{sgn}(\dot{x}) + \beta_5 \operatorname{sgn}(z) + \beta_6 \operatorname{sgn}(x)$$

Equation 6

Using the finite differences method (first order) applied to Equation the following iterative method was developed:

$$
\begin{cases}
z_0 = Initial\_Torque \\
x_0 = Initial\_Angle \\
z_{i+1} = (x_{i+1} - x_i)\left[A - |z|^n \Psi_i(x, \dot{x}, z)\right] + z_i \\
\Psi_i(x, \dot{x}, z) = \beta_1 \operatorname{sgn}[(x_{i+1} - x_i) z_i] + \beta_2 \operatorname{sgn}[(x_{i+1} - x_i) x_i] + \beta_3 \operatorname{sgn}[x_i z_i] \\
\qquad + \beta_4 \operatorname{sgn}[x_{i+1} - x_i] + \beta_5 \operatorname{sgn}[z_i] + \beta_6 \operatorname{sgn}[x_i]
\end{cases}
$$

Equation 7

Where *x* is the joint position angle and *z* is the corresponding torque.

This procedure allowed the following results:

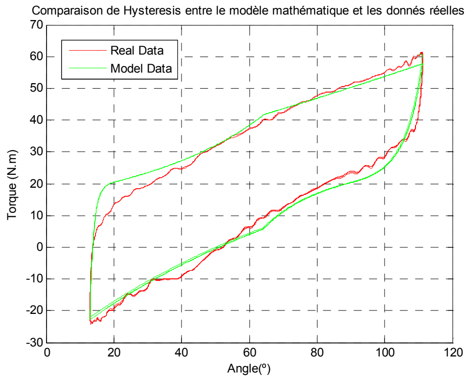

Figure 8 - Example of Hysteretic comparison between the mathematical model and real data

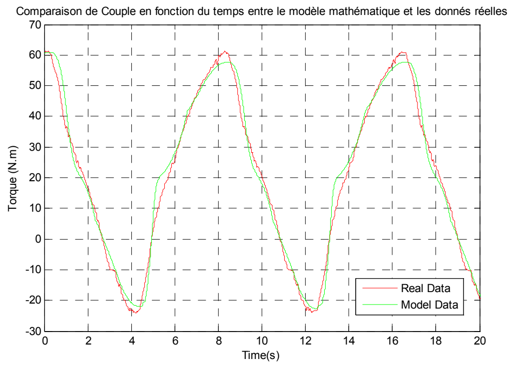

Figure 9 - Example of Torque comparison between the mathematical model results and real data

7. Conclusion

This article described the beginning of the development of a space suit simulator which intends to simulate all current and future spacesuits.

This simulator will allow a reduction of the planning procedures costs, a simplification of the training procedure of the astronauts and a better study of the influence of the various parameters of a spacesuit on the behavior of the astronaut.

Tools were created to the use of an anthropomorphic robot, to measure the behavior of the first joint of the simulator, the knee joint. The analysis of the results was detailed, namely the subtraction of torque due to the robot itself, data filtering and scaling, to arrive at results which allowed the characterization of this joint.

Physical and mathematical models allowed a validation of the results. The mathematical model used an innovative procedure that can also be applied to other systems with hysteretic behaviors.

The results of this study will allow a better prediction of the necessary torques to bend each joint of the simulator and, as the simulator will allow the simulation of all current and future spacesuits, the characteristics of each spacesuit can also be evaluated. The results of the models will, in the future, allow a better planning of the extravehicular activities (EVA) as well as a better definition of the astronaut's work envelope(i.e. range of joint positions where the astronaut feels more comfortable working at).